Pressure effects on the phase stability of cubic BNC ternary alloys

2009 J. Phys.: Condens. Matter 21 055403

(http://iopscience.iop.org/0953-8984/21/5/055403)

J. Phys.: Condens. Matter **21** (2009) 055403 (6pp) doi:10.1088/0953-8984/21/5/055403

Pressure effects on the phase stability of cubic BNC ternary alloys

Koretaka Yuge

Department of Materials Science and Engineering, Kyoto University, Sakyo, Kyoto 606-8501, Japan

Received 20 October 2008, in final form 15 December 2008
Published 12 January 2009
Online at stacks.iop.org/JPhysCM/21/055403

Abstract

Pressure effects on the phase stability of cubic BNC alloys were examined by Monte Carlo simulations and the cluster expansion technique based on first-principles calculations. At pressure $P = 10$ GPa, solution energy of neighboring B–N and C–C atoms into diamond and cubic BN are both higher than those at $P = 0$ GPa, indicating a decrease of solubility in c-BNC under applied pressure. Monte Carlo statistical simulation reveal that the applied pressure decreases solubility limits by almost half of those at $P = 0$ GPa. This significant decrease can mainly be attributed to the increase of volume with the formation of a c-BNC solid solution. Formation of neighboring B–N bonds decreases volume, while that of second-neighboring B–N increases volume for c-BNC, which naturally increases the stability of c-BN and diamond in the c-BNC solid solution under external pressure.

1. Introduction

Cubic boron nitride (c-BN) and diamond have outstanding physical properties such as a high melting point, hardness and bulk modulus [1, 2]. Due to the similarity of crystal structure and atomic sizes between C, B and N atoms, formation of a solid solution between c-BN and diamond, c-BNC, is naturally anticipated. The c-BNC ternary alloy hence becomes a promising material to show high hardness, and to show high thermal and chemical stability. With this stimulating background, a considerable number of experimental works have been devoted to synthesizing c-BNC under extreme conditions of temperature around $T = 2000$–3000 K and pressure around $P = 7$–20 GPa [1–5]. Despite the success of the synthesis of c-BNC, its thermodynamic stability has not been confirmed yet. Badzian [3] synthesized $(BN)_{(1-x)}(C_2)_x (0.4 \leqslant x \leqslant 0.85)$ solid solutions under a pressure of $P = 14.0$ GPa and a temperature of around $T = 3000$ K, and found a short-range order of the substitution of the B–N pair by the C–C pair along the 1-NN coordination. Nakano *et al* [4] obtained c-BNC with $x = 0.5$, $P = 7.7$ GPa and $T = 2000$–2400 K and concluded that c-BNC is not thermodynamically stable under these conditions and is likely to undergo phase separation into c-BN and diamond.

Meanwhile, a few theoretical investigations based on density functional theory (DFT) addressed the phase stability of c-BNC under atmospheric pressure ($P = 0$ GPa) [6–8]. However, these calculations employ rather simplified thermodynamic models compared to the recent theoretical approaches on phase diagrams on metal alloys [9–12], which should not be sufficient to confirm the stability of c-BNC. Very recently, Yuge *et al* [13] successfully made an accurate prediction of the phase stability of c-BNC based on DFT. They included the effects of lattice vibration, atomic-arrangement dependence of total energy and effects of atomic ordering on configuration entropy, which should be significant for an accurate calculation of phase diagrams [9, 10, 12]. They confirmed that: (i) no stable intermediate phase exists and c-BNC undergoes phase separation into c-BN and diamond, (ii) complete miscibility cannot be achieved below melting temperature T_m and (iii) the c-BNC solid solution shows a strong preference of neighboring B–N and C–C bonds and has almost no B–B and N–N bonds up to T_m. In [13], however, the phase stability of c-BNC was investigated under atmospheric pressure, while in the previous experiments, successful synthesis of the c-BNC is always performed under high pressure of around $P = 7$–20 GPa as described above. Therefore, further investigation including the effects of pressure should be required for practical assessment of the phase stability of c-BNC alloys.

In the present work, we focus on the phase stability of c-BNC along the composition range of $(BN)_{(1-x)}(C_2)_x$ $(0 \leqslant x \leqslant 1)$ which is naturally originated from the mixture of c-BN and diamond. The energetic of pressure effects on the phase stability of c-BNC is accurately treated using the cluster expansion (CE) technique based on DFT calculations in a

state-of-the-art manner [13, 14]. The resultant effective interactions are then applied to the Monte Carlo (MC) simulation to obtain statistical ensemble averages such as solubility limits.

2. Methodology

2.1. Cluster expansion technique

The CE technique is adopted to expand DFT energies. We start from the Gibbs free energy of a system with given atomic arrangement $\vec{\sigma}$ under external pressure P described as

$$G(P, \vec{\sigma}) = E_{\mathrm{el}}(V, \vec{\sigma}) + PV, \tag{1}$$

where E_{el} denotes the electronic contribution to the free energy and V represents the volume of the system. In equation (1), vibrational contributions to the Gibbs free energy are factored out.

The essence of the CE is an expansion of any property (here, $G(P, \vec{\sigma})$) in terms of the atomic arrangements. In this technique, we first define the variables $\sigma_i = \{+1, 0, -1\}$ that specify the occupation of B, C and N atoms at lattice point i in a heterodiamond structure, respectively. Using σ_i, we can construct functions that are complete and orthonormal for whole N lattice points [13]:

$$\begin{aligned} G(P, \vec{\sigma}) &= V_0\Phi_0 + \sum_n \sum_{(\tau)} V_n^{(\tau)} \Phi_n^{(\tau)}(\vec{\sigma}) \\ \Phi_n^{(\tau)} &= \phi_{\tau_1}\left(\sigma_{n_1}\right)\phi_{\tau_2}\left(\sigma_{n_2}\right)\ldots\phi_{\tau_n}\left(\sigma_{n_n}\right) \\ \phi_0(\sigma_i) &= 1 \\ \phi_1(\sigma_i) &= \sqrt{\tfrac{3}{2}}\sigma_i \\ \phi_2(\sigma_i) &= -\sqrt{2}\left(1 - \tfrac{3}{2}\sigma_i^2\right), \end{aligned} \tag{2}$$

where the expansion coefficient V is called an effective cluster interaction (ECI) that is independent of $\vec{\sigma}$, $\phi(\sigma_i)$ is the orthonormal basis function for lattice point i and Φ is called a cluster function obtained by products of ϕs. n specifies the set of lattice points whose basis function is not unity (i.e. $\neq\phi_0$), which corresponds to the cluster figure, and (τ) specifies the set of basis-function indexes described by the subscript to ϕ. We should note here that the contribution of E_{el} and PV in equation (1) can be individually expanded in the form of equation (2) since they are both functions of atomic arrangements $\vec{\sigma}$.

To determine the ECIs, we perform least-squares (LS) fitting of the total energies for c-BNC ordered structures obtained via DFT calculations under an external pressure of $P = 10$ GPa. Other calculation conditions are described in the previous paper [13]. Due to the limitation number of DFT input energies, expansion in equation (2) should be terminated at finite order. Therefore, we should choose an optimal set of clusters $\{n\}$ that give accurate prediction of energies for given atomic arrangements under $P = 10$ GPa. In the present work, we used clusters that are already optimized under atmospheric pressure. This is because the contribution of PV to the Gibbs free energy is additive compared to the electronic contribution E_{el}. In fact, the resultant cross-validation (CV) score [15, 16], which describes the uncertainty of the energies predicted by ECIs, is 6.7 meV/atom, which is the same order of CV score as 5 meV/atom under $P = 0$ GPa. We have confirmed that these CV scores give sufficient accuracy to express relative energetics of individual atomic arrangements for c-BNC.

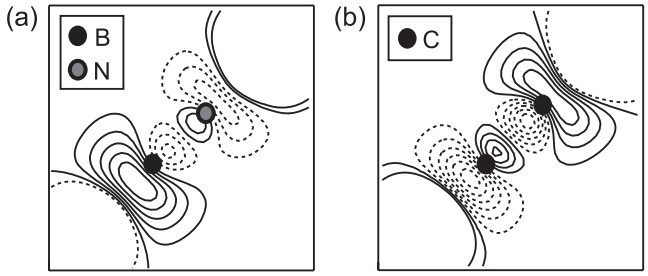

Figure 1. Contour plot of charge density for (a) neighboring B–N atoms in diamond measured from those in c-BN; (b) neighboring C–C atoms in c-BN measured from those in diamond. Solid and dotted curves represent increase and decrease of charge density, respectively.

2.2. Monte Carlo simulation

In order to obtain the configurational properties of c-BNC, Monte Carlo (MC) statistical thermodynamic simulations under grand-canonical ensembles are carried out on the Metropolis algorithm [17]. In the MC simulations, we used a $4 \times 4 \times 4$ expansion of the diamond structure unit cell under three-dimensional periodic boundary conditions, which is sufficient in terms of the cell-size dependence of the MC results. The other calculation conditions are described in detail in the previous paper [13].

3. Results and discussion

3.1. Trends of solubility in dilution limit

The previous paper [13] reveals that, at $P = 0$ GPa, (i) c-BNC has no stable intermediate phase and undergoes phase separation into c-BN and diamond and (ii) the c-BNC solid solution strongly favors neighboring B–N and C–C atoms up to melting temperature. These facts indicate that the c-BNC solid solution is interpreted as a random mixture of neighboring B–N and C–C atoms rather than that of B, C and N atoms. Therefore, we first consider a model of the dilution limit for the solid solution where single B–N (C–C) atoms solute into bulk diamond (c-BN) in order to investigate a trend of solubility in c-BNC. We performed DFT calculations on 64-atom supercells of diamond (c-BN) with two neighboring atoms replaced by B–N (C–C) atoms under $P = 0$ and 10 GPa. Figure 1 shows the contour plot of the resultant charge density for neighboring B–N (C–C) atoms in diamond (c-BN) measured from B–N (C–C) atoms in bulk c-BN (diamond) at $P = 0$ GPa. Solid and dotted curves represent the increase and decrease of charge density, respectively. It can be clearly seen that charge density for B–N and C–C markedly changes when they solute from bulk into diamond or c-BN, although c-BN with sp^3 structures

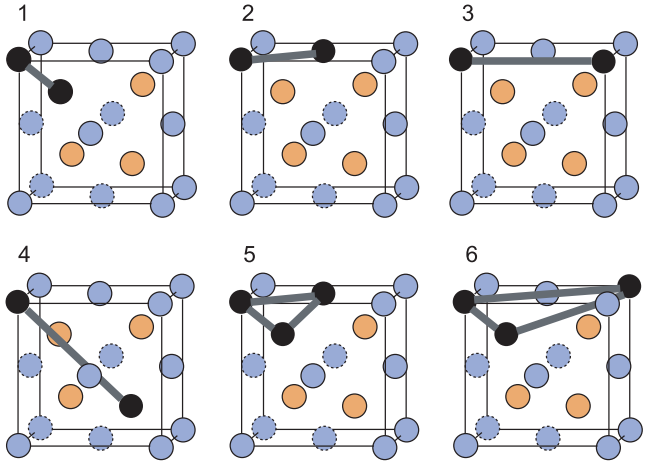

Figure 2. Selected multibody clusters in the heterodiamond structure.

(This figure is in colour only in the electronic version)

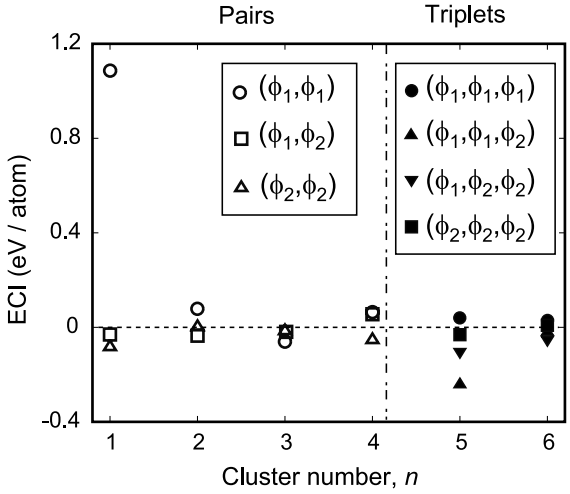

Figure 3. Effective cluster interactions for the multibody clusters under $P = 10$ GPa. Parentheses denote basis functions for each lattice point given by equation (2).

is isoelectronic to diamond. This can be naturally attributed to the change in local chemical environment around B, C and N atoms in the solid solution. For instance, the B atom in c-BN coordinates with four N atoms along the first-nearest neighbor (1-NN) while it coordinates with one N atom and three C atoms in the solution of B–N atoms in diamond. Since the electron energy level for C is higher than that for N, replacement of N by C atoms causes an increase of charge density near the B atom along the B–C bonds in 1-NN coordination, which can be seen in figure 1. The increase or decrease of charge density around N and C atoms in figure 1 can also be attributed to such changes in chemical environment.

Next, we investigate the energetic of pressure effects on solubility of B–N (C–C) atoms into diamond (c-BN). This can be done by introducing the solution energy of B–N (C–C) defined as

$$\Delta E^{\mathrm{sol}}_{\mathrm{BN(CC)}} = E^{\mathrm{dilute}}_{\mathrm{BN(CC)}} - (n_{\mathrm{BN}} E_{\mathrm{c-BN}} + n_{\mathrm{CC}} E_{\mathrm{diamond}}). \quad (3)$$

Here, $E^{\mathrm{dilute}}_{\mathrm{BN(CC)}}$ denotes total energy of the dilution limit model where diamond (c-BN) has two neighboring atoms replaced by B–N (C–C) atoms as described above, $E_{\mathrm{c-BN}}$ of bulk c-BN and E_{diamond} of bulk diamond. n_{BN} and n_{CC} represent the number of B–N and C–C atoms in the dilution limit model, respectively. Table 1 summarizes the calculated solution energy ΔE^{sol} under $P = 0$ and 10 GPa. At $P = 10$ GPa, 'no PV' denotes the contribution from the electronic part, E_{el} in equation (1), and 'with PV' denotes the contribution from $E_{\mathrm{el}}+PV$. Parentheses denote solution energies measured from that at $P = 0$ GPa for C–C or B–N atoms, respectively. At $P = 0$ GPa, solution energy for both B–N and C–C atoms exhibits a positive sign, which supports the tendency of phase separation into c-BN and diamond. Another notification is that the solution energy for B–N atoms is 0.17 eV larger than that for C–C, indicating that solubility of B–N into diamond is smaller than that of C–C into c-BN in the dilution limit. In fact, the previous calculation [13] showed a smaller solubility for the diamond-rich composition compared to that for the c-BN-rich composition. Therefore, our model of the dilution limit certainly describes a qualitative trend of solubility in c-BNC. When a pressure of 10 GPa is applied, solution energies increase both for B–N and C–C. Comparing E^{sol} at $P = 10$ GPa with a PV term with that at $P = 10$ GPa without a PV term, the increase of solution energy mainly comes from the PV contribution, and the electronic part E_{el} is a predominant contribution. Therefore, one can predict a decrease of solubility for both B–N and C–C atoms under external pressure, due mainly to the increase in volume V with the formation of a c-BNC solid solution. However, quantitative estimation of solubility should require more accurate treatment of Gibbs free energy depending on atomic arrangements and composition in c-BNC, which will be discussed in the following sections.

Table 1. Calculated solution energies ΔE^{sol} (in eV) for neighboring B–N and C–C atoms into diamond and c-BN, respectively.

	0 GPa	10 GPa (no PV)	10 GPa (with PV)
C–C in c-BN	2.69	2.70 (+0.01)	2.74 (+0.05)
B–N in diamond	2.86	2.88 (+0.02)	2.92 (+0.06)

3.2. Effective cluster interactions for c-BNC

Figure 2 shows the selected six multibody clusters used for the present c-BNC system; four pairs in 1-, 2-, 3- and 6-NN coordination, and two triplets. In addition to the six multibody clusters, one empty and point clusters are used. The corresponding ECIs are shown in figure 3. We can see the dominant contribution of the 1-NN pair cluster with basis functions (ϕ_1, ϕ_1), and the ECIs rapidly converge with respect to the interatomic distances. The same trend of convergence can also be seen for triplets; clusters of smaller size (cluster no. 5) have larger ECIs than those of larger size (cluster no. 6) for each basis-function set.

While these ECIs for pairs have explicit interpretation of coefficients of the orthonormal expansion in equation (2), they do not give any intuition of which atomic bonds are likely

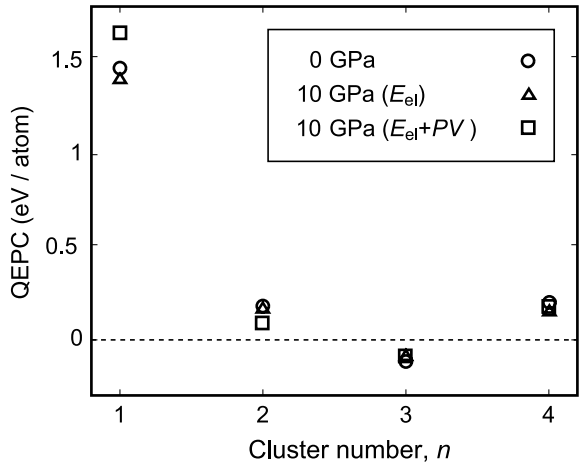

Figure 4. Calculated quasibinary effective pair contributions (QEPCs) for B–N pairs under $P = 0$ and 10 GPa.

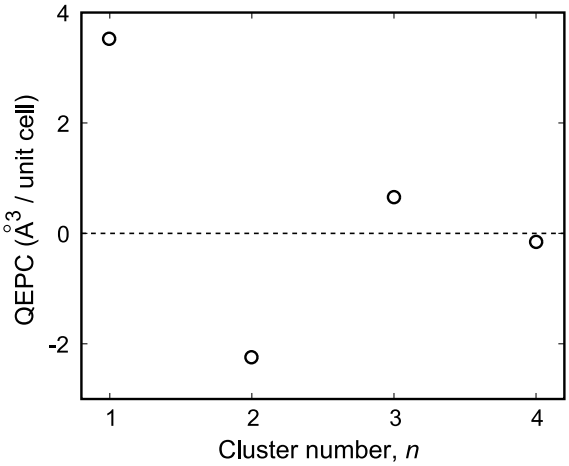

Figure 5. Calculated quasibinary effective pair contributions (QEPCs) of volume for B–N atoms under $P = 0$ GPa.

to be preferred or not. Thus we project orthonormal basis functions Φ onto cluster-probability basis functions, which have a transparent interpretation in terms of the ordering tendency [18]. Note that, since the cluster-probability basis is not orthonormal, we use them just for seeing the trends of preference for atomic bonds. Using the cluster-probability basis, the contribution of pair clusters to the Gibbs free energy can be simply given by

$$G_{\text{pair}}(\vec{\sigma}, V) = -4 \sum_{\text{pairs}}^{i} [W^i_{\text{IJ}} \chi^i_{\text{IJ}} + W^i_{\text{JK}} \chi^i_{\text{JK}} + W^i_{\text{IK}} \chi^i_{\text{IK}}], \quad (4)$$

where χ^i_{IJ} denotes the probability basis for pair cluster i with I–J atoms, and W^i_{IJ} the corresponding coefficients, which are called quasibinary effective pair contributions (QEPCs). The QEPC, W, can be expressed by a linear combination of the ECIs [13] and has an explicit form of

$$W^i_{\text{IJ}} = \tfrac{1}{4}[G_{\text{II}} + G_{\text{JJ}} - G_{\text{IJ}} - G_{\text{JI}}], \quad (5)$$

where G_{IJ} denotes the average Gibbs free energy of all the atomic arrangements in a ternary system with I and J atoms in pair cluster i. Therefore, $W_{\text{IJ}} > 0$ corresponds to a preference of I–J unlike atom pairs with respect to I–I and J–J like atom pairs, and $W_{\text{IJ}} < 0$ to a disfavor of I–J atom pairs. In the present c-BNC ternary alloy, we have three QEPCs for B–C, C–N and B–N atoms. Here we focus on the QEPCs for B–N atoms because (i) they give direct interpretation of the phase separation in terms of the preference of B–N atoms and its counterpart for C–C atoms and (ii) QEPCs for B–N atoms have a dominant contribution in c-BNC. The resultant QEPCs under $P = 0$ and 10 GPa are shown in figure 4. Open circles denote QEPCs under $P = 0$ GPa, open triangles the electronic contribution E_{el} under $P = 10$ GPa and open squares $E_{\text{el}} + PV$ under $P = 10$ GPa. For pressures of both $P = 0$ and 10 GPa, the dominant contribution comes from the 1-NN pair. The positive sign of QEPCs along 1-NN indicates the strong preference of B–N atoms, which supports the trends of phase separation. QEPCs along 2-NN have smaller positive signs, which should slightly weaken the stability of c-BN in a c-BNC solid solution. When pressure is applied, we can see that the electronic contribution E_{el} slightly decreases QEPC along 1-NN by 0.06 eV per atom, while the PV contribution markedly increases QEPC by 0.25 eV. In contrast, applied pressure decreases QEPC along 2-NN by 0.03 eV. These facts indicate that applied pressure increases the preference of neighboring B–N atoms while it decreases the preference of second-neighboring B–N atoms due mainly to the contribution of PV. These trends of preferences certainly increase the stability of c-BN and diamond in a c-BNC solid solution, resulting in a decrease of solubility for both c-BN and diamond. In order to see the dominant contribution of PV to the decrease of solubility, volume V at $P = 0$ GPa is expanded in a similar way to Gibbs free energy in equation (2). The resultant QEPCs of volume for B–N atoms are shown in figure 5. The dominant contribution comes from the first- and second-neighboring B–N atoms. It can be clearly seen that, at $P = 0$ GPa, QEPC along 1-NN has a positive value, indicating that neighboring B–N atoms decrease the volume, while second-neighboring B–N atoms increase the volume. These facts indicate that formation of a c-BNC solid solution always results in an increase of volume because the number of neighboring B–N atoms should decrease while that of second-neighboring B–N atoms increases [13].

Figure 6 shows the calculated volume for disordered c-BNC alloy at $T = 4500$ K under $P = 0$ GPa using ECIs for the volume. The volume for the c-BNC solid solution certainly shows positive deviation by $\sim$1% from the ideal mixing (Vegard's law), which is in excellent agreement with the previous experimental report of 1% positive deviation in volume [1]. To summarize, external pressure increases the Gibbs free energy through the PV term due to the increase of volume with formation of c-BNC solid solution; this decreases the solubility of c-BN and diamond under pressure.

3.3. Phase diagram of c-BNC under high pressure

A quantitative estimation of solubility limits can be done by applying the ECIs in figure 3 to MC statistical simulation

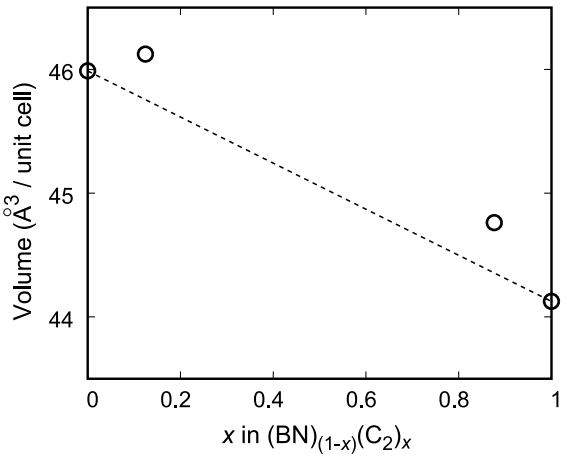

Figure 6. Calculated volume per diamond unit cell for disordered c-BNC alloy at $T = 4500$ K under $P = 0$ GPa.

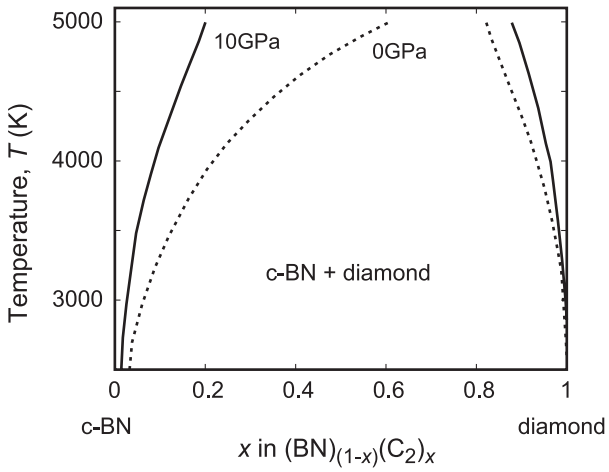

Figure 7. Calculated phase diagram for c-BNC along the composition range of $(BN)_{(1-x)}(C_2)_x$ $(0 \leqslant x \leqslant 1)$. The dotted curves denotes solubility limits under $P = 0$ GPa and the solid curves those under $P = 10$ GPa.

under a grand-canonical ensemble. Here, we consider the composition range of $(BN)_{(1-x)}(C_2)_x$ $(0 \leqslant x \leqslant 1)$. Therefore, exchange of BN and C_2 atoms between the MC simulation box and the thermal bath should be taken into account. The input chemical potential in the grand-canonical MC simulation thus becomes the difference between that of BN and C_2:

$$\Delta\mu = \mu_{BN} - \mu_{C_2}. \tag{6}$$

In order to obtain the phase diagram in the grand-canonical MC simulation, the composition x should be estimated as a function of $\Delta\mu$. During the MC simulation, we first increase the chemical potential $\Delta\mu$ discretely from -0.16 to 0.72 eV, then decrease $\Delta\mu$ from 0.72 to -0.16 eV. The resultant $\Delta\mu$–x curve should show a hysteresis between the increase and decrease of $\Delta\mu$, because a phase-separating system typically requires a driving force for a drastic change in composition due to the phase coexistence, which should correspond to finite excess of chemical potential from the equilibrium state in the grand-canonical MC simulation [13]. We can then estimate the solubility limits from the hysteresis curve, which is described in detail in the previous paper [13]. Errors of the estimated solubility limits due to using the hysteresis curve are within $\pm 0.8\%$ of composition throughout the temperature in figure 7.

Applying the simulation on the $\Delta\mu$–x curve, we can finally obtain the phase diagram of c-BNC shown in figure 7. The dotted curves denote solubility limits under $P = 0$ GPa [13] and the solid curves those under $P = 10$ GPa. A significant decrease of solubility limits can be seen under the pressure of $P = 10$ GPa, which can also be predicted by the QEPCs discussed in section 3.2. At $T = 4000$ K near the melting point of diamond ($T_m \sim 4100$ K at $P = 12.5$ GPa) [19], solubility limits for both c-BN and diamond decrease by around half under $P = 10$ GPa; at $P = 0$ GPa, solubility limits of c-BN and diamond are estimated to be $\sim 22\%$ and $\sim 7\%$, while at $P = 10$ GPa those of c-BN and diamond are estimated to be $\sim 9\%$ and $\sim 4\%$, respectively. These facts suggest that the previous success in synthesis of c-BNC compounds is due to the kinetic reason under extreme high temperature and pressure but not to a reason of the energetic in thermodynamic equilibrium in c-BNC.

4. Conclusions

Pressure effects on the phase stability of c-BNC along a composition range of $(BN)_{(1-x)}(C_2)_x$ $(0 \leqslant x \leqslant 1)$ is examined by the combination of the cluster expansion technique and Monte Carlo simulation based on first-principles calculations. When neighboring B–N and C–C atoms solute from bulk into diamond and c-BN, the corresponding charge density significantly changes due to the change in local chemical environment. In c-BNC, the estimated QEPCs indicate a strong preference of the B–N bond along the 1-NN coordination at both $P = 0$ and 10 GPa, which supports the trends of phase separation of c-BNC into c-BN and diamond. Applied pressure increases the preference of neighboring B–N atoms while it decreases that of second-neighboring B–N atoms, due mainly to the contribution of the PV term to the Gibbs free energy. This can be related to the decrease and increase of volume when neighboring and second-neighboring B–N atoms are formed in c-BNC. These facts indicate the decrease of solubility for both B–N and C–C atoms under external pressure, due to the increase in volume V with the formation of a c-BNC solid solution. Using the MC statistical simulation under grand-canonical ensemble, a c-BNC phase diagram is constructed. When a pressure of $P = 10$ GPa is applied, solubility limits of both c-BN and diamond markedly decreased by half of those at $P = 0$ GPa near the melting point of diamond. These facts suggest that the success in synthesis of c-BNC compounds under high pressure should relate to the kinetic reason, but not to a reason of the energetic in thermodynamic equilibrium.

Acknowledgments

This research was supported by a Grant-in-Aid for the Global COE Program, 'International Center for Integrated Research and Advanced Education in Materials Science,' from the Ministry of Education, Culture, Sports, Science and

Technology of Japan. The author express cordial thanks to Dr Fumiyasu Oba and Dr Yukinori Koyama for giving fruitful suggestions for the present work.

References

[1] Knittle E, Kaner R B, Jeanloz R and Cohen M L 1995 *Phys. Rev.* B **51** 12149
[2] Solozhenko V L, Andrault D, Fiquet G, Mezouar M and Rubie D C 2001 *Appl. Phys. Lett.* **78** 1385
[3] Badzian A R 1981 *Mater. Res. Bull.* **16** 1385
[4] Nakano S, Akaishi M, Sasaki T and Yamaoka S 1996 *Chem. Mater.* **6** 2246
[5] Komatsu T, Nomura M, Kakudate Y and Fujisawa S 1996 *Mater. Chem.* **6** 1799
[6] Lambrecht W R L and Segall B 1993 *Phys. Rev.* B **47** 9289
[7] Zheng J C, Huan C H A, Wee A T S, Wang R and Zheng Y 1999 *J. Phys.: Condens. Matter* **11** 927
[8] Zheng J C, Wang H Q, Wee A T S and Huan C H A 2002 *Phys. Rev.* B **66** 092104
[9] van de Walle A and Ceder G 2002 *Rev. Mod. Phys.* **74** 11
[10] Yuge K, Seko A, Kuwabara A, Oba F and Tanaka I 2006 *Phys. Rev.* B **74** 174202
[11] Yuge K, Seko A, Tanaka I and Nishitani S R 2005 *Phys. Rev.* B **72** 174201
[12] Ozoliņš V, Wolverton C and Zunger A 1998 *Phys. Rev.* B **58** R5897
[13] Yuge K, Seko A, Koyama Y, Oba F and Tanaka I 2008 *Phys. Rev.* B **77** 094121
[14] Blum V and Zunger A 2004 *Phys. Rev.* B **70** 155108
[15] Stone M 1974 *J. R. Stat. Soc.* B **36** 111
[16] Allen D M 1974 *Technometrics* **16** 125
[17] Metropolis N, Rosenbluth A W, Rosenbluth M N, Teller A H and Teller E 1953 *J. Chem. Phys.* **21** 1087
[18] Wolverton C and Fontaine D 1994 *Phys. Rev.* B **49** 8627
[19] Madelung O 1987 *Landolt–Börnstein* (*New Series* Group III, Pt. a, vol 22) (Berlin: Springer)